



A geospatial approach for assessing urban flood risk zones in Chennai, Tamil Nadu, India

Murugesan Bagyaraj¹ · Venkatramanan Senapathi² · Sang Yong Chung³ · Gnanachandrasamy Gopalakrishnan⁴ · Yong Xiao⁵ · Sivakumar Karthikeyan² · Ata Allah Nadiri^{6,7,8} · Rahim Barzegar⁹

Received: 9 January 2023 / Accepted: 29 July 2023 / Published online: 28 August 2023
© The Author(s), under exclusive licence to Springer-Verlag GmbH Germany, part of Springer Nature 2023

Abstract

Chennai, the capital city of Tamil Nadu in India, has experienced several instances of severe flooding over the past two decades, primarily attributed to persistent heavy rainfall. Accurate mapping of flood-prone regions in the basin is crucial for the comprehensive flood risk management. This study used the GIS-MCDA model, a multi-criteria decision analysis (MCDA) model that incorporated geographic information system (GIS) technology to support decision making processes. Remote sensing, GIS, and analytical hierarchy technique (AHP) were used to identify flood-prone zones and to determine the weights of various factors affecting flood risk, such as rainfall, distance to river, elevation, slope, land use/land cover, drainage density, soil type, and lithology. Four groups (zones) were identified by the flood susceptibility map including high, medium, low, and very low. These zones occupied 16.41%, 67.33%, 16.18%, and 0.08% of the area, respectively. Historical flood events in the study area coincided with the flood risk classification and flood vulnerability map. Regions situated close to rivers, characterized by low elevation, slope, and high runoff density were found to be more susceptible to flooding. The flood susceptibility map generated by the GIS-MCDA accurately described the flood-prone regions in the study area.

Keywords AHP technique · Remote sensing · GIS-MCDA · DEM · Flood risk factors · Flood susceptibility map

Responsible Editor: Philippe Garrigues

✉ Sang Yong Chung
chungsy@pknu.ac.kr

Venkatramanan Senapathi
venkatramanansenapathi@gmail.com

Gnanachandrasamy Gopalakrishnan
samynanam@gmail.com

Yong Xiao
xiaoyong@swjtu.edu.cn

Ata Allah Nadiri
Nadiri.ata@gmail.com

Rahim Barzegar
Rahim.Barzegar@uqat.ca

³ Department of Earth and Environmental Sciences, Pukyong National University, Busan 48513, South Korea

⁴ Department of Earth Sciences, School of Physical, Chemical, and Applied Sciences, Pondicherry University, Puducherry 605014, India

⁵ Faculty of Geosciences and Environmental Engineering, Southwest Jiaotong University, SWJTU Xipu Campus, Chengdu 611756, China

⁶ Department of Earth Sciences, Faculty of Natural Sciences, University of Tabriz, Tabriz, Iran

⁷ Institute of Environment, University of Tabriz, Tabriz, Iran

⁸ Traditional Medicine and Hydrotherapy Research Center, Ardabil University of Medical Sciences, Ardabil, Iran

⁹ Groundwater Research Group (GRES), Research Institute on Mines and Environment (RIME), Université du Québec en Abitibi-Témiscamingue (UQAT), Amos, Québec, Canada

¹ Department of Geology, College of Natural and Computational Sciences, Debre Berhan University, P.O. Box 445, Debre Berhan, Ethiopia

² Department of Geology, Faculty of Science, Alagappa University, Karaikudi 630003, Tamil Nadu, India

Introduction

Floods pose a significant threat to human life and properties, making them one of the most destructive calamities in nature (Ghosh and Kar 2018; Joy et al. 2019). Industrialization, urbanization and climate change (Detrembleur et al. 2015; Khosravi et al. 2020; Tabari 2020) have led to an increase in floods (Barasa and Perera 2018; Muthusamy et al. 2018). It is an unavoidable natural occurrence that is expected to worsen the human life in the future (Yukiko et al. 2021) and to threaten many regions around the globe. The present and future flood susceptibility scenarios require a large amount of spatial and temporal data on the prediction of prospective flooding risks (de Moel et al. 2015). Flood risk assessment, identification of flood-prone areas, and implementation of appropriate management and mitigation measures are critical to reducing flood-related vulnerability and losses. Flood susceptibility mapping is valuable for flood susceptibility reduction plans, early warning systems, and emergency response strategies (Vieri et al. 2020).

In flood risk analysis, numerical models are often used to measure flood risk (Kuldeep Garg and Garg 2016; Zhang and Chen 2019). Hydrological and hydrodynamic models have been widely used to determine flood magnitude, extent, and frequency (Ullah et al. 2016). For example, rainfall-runoff modeling and flow routing modeling have been employed for predicting flooding (Sindhu and Durga Rao 2017; Liu et al. 2018), along with the runoff yield model, a type of hydrological model, to analyze the flood pathway in the flow channels (Chomba et al. 2021). These models can handle large quantities of data and provide useful flood information. However, Cabrera and Lee (2019) pointed out that hydro-meteorological data shortage is the most problematic and prevalent aspect of such systems. Furthermore, flood risk assessment is a difficult task in India due to the deficiency of quality data. As a result, the development of a robust flood risk analysis model is necessary to overcome this limitation.

Geographical information system (GIS) is widely used in flood risk assessment and management because of its ability to process and analyze large data sets, including hydrological and meteorological data, digital elevation model (DEM), and land use data. A key advantage of GIS for this purpose is its ability to allow the integration of multiple data sources, such as satellite imagery and topographic maps, and to produce comprehensive flood susceptibility maps for decision making. In addition, GIS technology can be used to simulate flooding events and to predict their potential impacts. The effectiveness of flood control measures can also be evaluated using GIS. The integration of GIS into flood risk assessment

and management has proven to be an effective approach to identify flood-prone areas, predicting potential flood scenarios, and evaluating the effectiveness of mitigation measures (Areu-Rangel et al. 2019; Dash and Sar 2020; Chomba et al. 2021; Kongeswaran and Sivakumar 2022).

Several research publications (Wu et al. 2015; Xiao et al. 2017) have examined the impacts of variables affecting flooding through the utilization of multi-criteria decision analysis (MCDA) and GIS. The GIS-MCDA strategy, which combines the GIS's geographic data processing capabilities with MCDA's capacity to link realistic data (such as precipitation, slope, drainage density, soil, and land use) to decision-based information, has been shown to be effective (Kazakis et al. 2015; Gigovic et al. 2017; Seejata et al. 2018; Kongeswaran and Sivakumar 2022).

The GIS-MCDA model was applied to investigate the difficult decision dilemmas under hierarchically grouped regulating factors (Rimba et al. 2017). According to De Brito and Evers (2016), most studies involving GIS-based MCDA paired it with the analytical hierarchy process (AHP). The AHP method allows many parameters to be broken down into a series of pairwise comparisons, following which the results can be combined (Saaty 2014). Several multidisciplinary studies on natural susceptibility assessment, such as flood susceptibility mapping, soil erosion susceptibility mapping (Kachouri et al. 2015), landslide susceptibility mapping (Feizizadeh et al. 2013), and groundwater potential zonation studies, have proven that GIS with AHP can be accomplished effectively within MCDA (Feizizadeh et al. 2013; Prabakaran et al. 2020; Arshad et al. 2020). The effectiveness of this strategy (i.e., integrating GIS and AHP in the MCDA framework) in susceptibility mapping is primarily stems from its ability to deal with the limited amount of data available (Cabrera and Lee 2019). The most commonly used features in flood susceptibility mapping are precipitation, distance to the river, DEM, slope, land use/land cover (LULC), drainage density, soil, and lithology. These features are often chosen after thorough literature reviews, and their weighting is determined using AHP method, which relies on expert knowledge (Naghbi et al. 2015; Mallick et al. 2019; Arshad et al. 2020; Kumar et al. 2020).

The present study aims to develop a mesoscale regional flood risk map for the Chennai district in Tamil Nadu, India using remote sensing data and GIS-MCDA model. Chennai has been more frequently affected by floods due to cyclonic rainfall from the Bay of Bengal region. The Chennai cloud-burst in 2015 was a severe weather event that caused widespread flooding and damage, resulting in an estimated 250 casualties. Therefore, creating a flood susceptibility map is important to manage future events. In this study, the GIS-AHP technique is also used to include eight criteria: rainfall (mm), distance to river (km), DEM (m), slope (%), LULC,

drainage density (km/km^2), soil type, and lithology. Based on the results of this study, managers and policy makers can gain a more comprehensive knowledge and specific recommendations regarding early warning systems, emergency response, and flood risk reduction measures.

Study area

The study was carried out in Chennai, the capital city of Tamil Nadu in India. Chennai district, previously known as Madras district, one of the 38 districts in Tamil Nadu and has the highest population density in the state, despite having the smallest area. Moreover, it encompasses the majority of Greater Chennai, which was previously divided among the districts of Tiruvallur, Kanchipuram, and Chengalpattu. Chennai is located at latitudes (13.0° N and 13.1° N) and longitudes (80.16° E to 80.3° E) (Fig. 1) with a total area of 426 km^2 . The region has the typical oppressive tropical climate, with most of the year being characterized by hot weather. The temperature in Chennai ranges from 26 to 35° C , and the average annual rainfall is 1400 mm . The northeast monsoon winds bring the most rainfall between September and December, usually triggered by cyclones in the Bay of Bengal. Rainfall during the southwest monsoon is highly erratic, and summer rains are barely noticeable (CCC&AR and TNSCCC 2015). The geology of the area is divided into four main lithological groups, including the

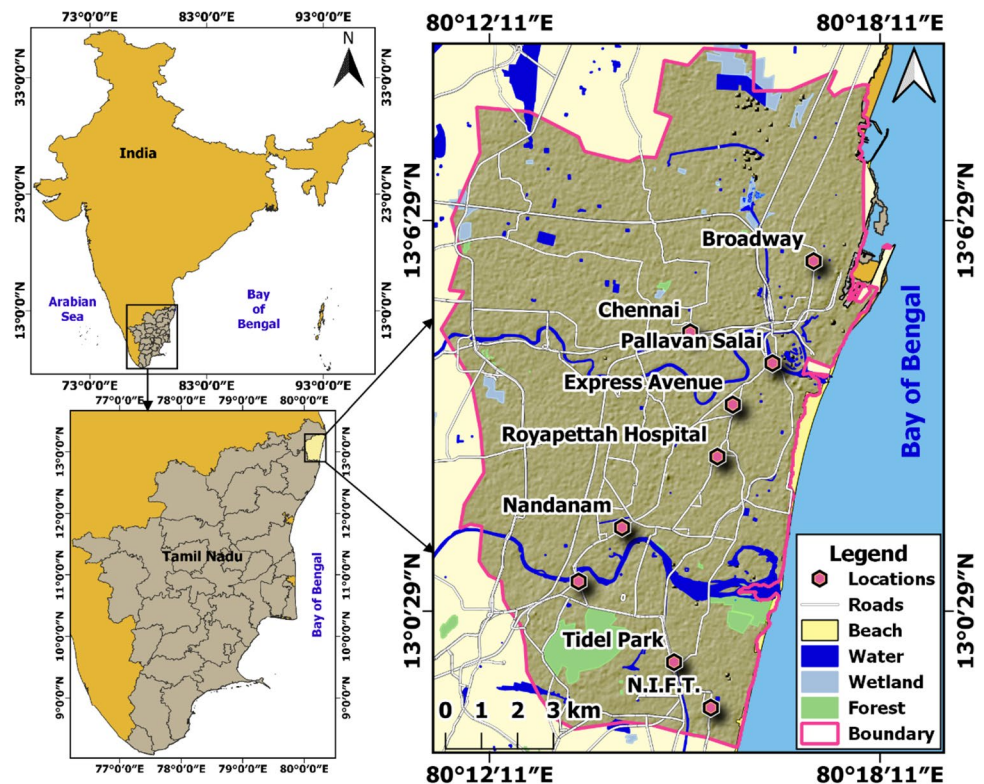
Archean chornockite, sandstone with conglomerate, sand with silt, and younger sand deposits formed by coastal, alluvial, and eolian processes. Both the higher-lying soils/alluvium and the eroded crystalline rocks in this region contain groundwater in the unconfined state. The maximum depth of drilled boreholes in the area is about 100 m .

Material and methods

Selection of flooding susceptibility factors

To assess vulnerability to flooding, various factors that trigger and cause flooding, along with their interactions, should be studied (Radmehr and Araghinejad 2015; Sahana and Patel 2019). Previous studies that mapped flood vulnerability have used a variety of flood regulatory elements, including precipitation, distance to river, elevation, slope, LULC, drainage density, soils, and lithology (Dou et al. 2018; Samanta et al. 2018; Das 2019). Despite the lack of consistency in the selection of flood regulating elements and their importance, researchers select the flood regulating factors based on physical and natural features. To create the flood susceptibility map, we used several satellite images and supplementary data sets from the Internet. The ArcGIS 10.3.1 “Reclassify” feature in the Spatial Analyst tools was used to convert the layers to a raster format and classify them.

Fig. 1 Map showing research site, Tamil Nadu



According to the literature review, the amount of precipitation plays an important role in flood formation. The annual mean rainfall for the study region from 2020 to 2021 was obtained from the Climate Research Unit (<https://chrsdata.eng.uci.edu/>). A total of five rain gauge stations were located at the following sites: (1) DGP Office, Mylapore; (2) Perambur Corporation Park; (3) Chennai collectorate building Pursawalkam V.O.C Nagar; (4) Sholinganallur; and (5) CD Hospital, Tondiarpet and were monitored. Using the “Conversion Tools”, “From Raster”, and “Raster to Point” options, the raster layer was converted to point values. The points were then loaded into “Spatial Analyst Tools”, “Interpolation”, and “IDW” to create the precipitation map of the watershed. We also considered the distance to rivers as a relevant criterion, given that floods are associated with the expansion of river networks. The Euclidean distance tool in ArcGIS 10.3.1 was used to calculate the distance to the river and divide the area into five zones.

Elevation serves as a fundamental representation of topographic features. DEM has been used as a critical evaluation criterion in several flood vulnerability assessment studies. Therefore, elevation constituted an important component of this study. DEM data of Chennai were acquired using EARTHDATA Search (<https://search.earthdata.nasa.gov/search>), where the “Advanced Spaceborne Thermal Emission and Reflection Radiometer (ASTER) Global DEM V003” was selected. The 30-m resolution images were retrieved from the (ASTER) Global DEM data and subsequently mosaicked using ArcGIS 10.3.1. This unified map was then re-projected based on the appropriate UTM zone.

In the current study, slope—a measure of the difference in elevation between adjacent grid cells— was selected as another flood-triggering feature due to its influence on flow velocity (Wu et al. 2015). ASTER DEM data were used to determine the basin slope in ArcGIS 10.3.1.

The LULC process directly affects flood interception, infiltration, subsurface infiltration, and evapotranspiration (Yan et al. 2013; Deng et al. 2015) and also has indirect impact on flooding (Rahman et al. 2019). LULC was chosen as another key element in the hierarchy. LULC data were obtained from Earth Explorer land cover data (<https://earthexplorer.usgs.gov/>). The “Land Cloud Cover” and “Scene Cloud Cover” criteria were set to less than 10% to obtain images with minimal cloud cover. These images were imported into ERDAS IMAGINE 2014 for processing and enhancement. For LULC classification, we used the supervised classification method in ERDAS IMAGINE. Maximum likelihood classification was utilized for land use mapping. This supervised classification process involves the selecting and digitizing polygons within an “area of interest” layer to create signature files. Multiple polygons

were created for each LULC category for classification. Supervised classification takes longer than unsupervised classification, and the overall accuracy of the land use map is 80%.

The drainage density of a landscape affects the flow path and the probability of flooding, leading to an appropriate concentration time of runoff. In this study, the density tool in ArcGIS 10.3.1 was employed to calculate drainage density. Soil properties affect the water retention capacity of the region, subsequently impacting water infiltration and flood risk (Rahmati et al. 2016a, 2016b). Therefore, soil parameters were considered as an additional factor in the current study.

A soil map of the watershed was provided by the Food and Agriculture Organization (FAO) GeoNetwork Web Portal. The SWAT Soil Repository was also used to determine soil types. The soil map was then georeferenced in ArcGIS 10.3.1 using the appropriate UTM coordinate system. It was then geocoded according to soil categories from SWAT. Flooding can be enhanced or reduced by lithology, as it affects water infiltration capacity and thus vulnerability to flooding. The GIS created a lithologic map of the study area at a 1/50,000 resolution based on the lithology present in the study area.

Analytic hierarchy process (AHP)

In the present work, remote sensing and GIS data are collected in order to generate a flood susceptibility map. This map is created based on eight regulatory criteria. Using the thematic maps of these components based on normalized weights, the AHP method was used to estimate flood susceptibility maps for the Chennai district. Assessing matrix consistency, scientific knowledge, and persuasive evidence are all fundamental to the implementation of AHP (Saaty 2014). The AHP technique follows the approach of Ghosh and Kar (2018), in which flood susceptibility variables are selected, relative scores are assigned, a pairwise comparison matrix is generated, and the matrix consistency is verified.

The pairwise comparison matrix was established following Saaty (1980), and the accuracy of the matrix was validated using the following formulas (Eqs. 1 to 5). Table 2 provides the standardized principal eigenvector. The scalar factor modifications resulting from a linear transformation affecting a vector are generally described by the eigenvalue (λ). Equation 4 was used to calculate the greatest estimated eigenvalues across all layers. C_i is the consigned indication value. The weight W_i is assigned to each measure in the pairwise comparison matrix. The consistency judgment factor is denoted as C_j . The largest eigenvalue is calculated using the formula λ_{\max} . In total, there are n criteria. The consistency index, random index, and consistency ratio

of the derived weights are abbreviated as CI, RI, and CR, respectively (Saaty 1980). The generated RI was followed as proposed by Saaty (1980) (Brunelli 2015; Agastheeswaran et al. 2021).

$$W_i = \frac{\sum_{i=1}^n \left[\frac{C_i}{\sum_{i=1}^n C_i} \right]}{n} \tag{1}$$

$$C_j = \frac{\sum_{i=1}^n [C_i \times W_i]}{W_i} \tag{2}$$

$$\lambda_j = \frac{\sum C_j}{n} \tag{3}$$

$$CI = \frac{\lambda_{max} - n}{n - 1} \tag{4}$$

$$CR = \frac{CI}{RI} \tag{5}$$

Pairwise comparison matrix

A range of professionals was surveyed in this study, including hydrologists, geomorphologists, remote sensing

Table 1 The significance of variables on a scale of 1–9 (Saaty 1980)

Strength of importance	Explanation
1	Equal significance
3	Medium significance
5	Strong
7	Very strong significance
9	Maximum significance
2, 4, 6, and 8	Intermediate between two adjacent values

Table 2 A (8×8) pairwise comparison matrix for the AHP-based flood susceptibility mapping

Matrix	RF	DR	DEM	SP	LULC	DD	SL	LY	NPEV
RF	1	3	8	2	9	3	7	8	35.23%
DR	1/3	1	3	8	2	5	5	5	23.79%
DEM	1/8	1/3	1	1	3	7	3	3	10.90%
SP	1/2	1/8	1	1	3	7	3	5	12.28%
LULC	1/9	1/2	1/3	1/3	1	7	3	2	7.81%
DD	1/3	1/5	1/7	1/7	1/7	1	4	2	4.36%
SL	1/7	1/5	1/3	1/3	1/3	1/4	1	2	3.02%
LY	1/8	1/5	1/3	1/5	1/2	1/2	1/2	1	2.61%
SUM									100%

*RF, rainfall; DR, distance to river; DEM, digital elevation model; SP, slope; LULC, land use/land cover; DD, drainage density; SL, soil; LY, lithology; NPEV, normalized principal eigen vector

specialists, and engineers. The tabular questionnaires were given to all experts to record their risk assessments of flood danger. Experts were requested to evaluate individual parameters (e.g., rainfall) against the others (which parameter is more significant?). Using the Saaty scale (Table 1), each parameter was scored based on its importance. Table 2 outlines eight factors contributing to floods (i.e., rainfall, lithology, drainage density, DEM, LULC, slope, soil, and distance to the river). Goepel (2013) merged these tables into an Excel template (<https://bpmmsg.com/new-ahp-excel-templatewith-multiple-inputs/>). The flood susceptibility mapping template generates a pairwise comparison matrix (8×8) for AHP-based flood susceptibility mapping (Table 2). A CR of 1.4% (less than 10%) is deemed acceptable for conducting the weighted overlay calculations to incorporate the weighted parameters.

Identification of flood susceptibility zones

Weighting values were assigned to the levels and classes based on their significance to flood risk. The levels/classes were weighted according to expert knowledge (Tables 2 and 3). The final score was calculated by simply weighing the classes. Each pixel of the output map (H_i) is calculated using the following equation (Das 2019):

$$H_i = \sum (W_j \times X_{ij}) \tag{6}$$

where W_j is j parameter weight and X_{ij} is class rank.

Results and discussion

Flood susceptibility mapping by AHP

Eight thematic layers (e.g., rainfall, distance to river, elevation, slope, LULC, drainage density, soil, and lithology) were established to depict flood susceptibility

Table 3 Assigned weight and rank scores for the layer/class of the Chennai district

Parameter (unit)	Class	Flood susceptibility	Parameter weight (%)	Class rank
Rainfall (mm/year)	100–200	Very low	35.23	1
	200–300	Low		2
	300–400	Moderate		3
	400–500	High		4
	> 500	Very high		5
Distance to the river (km)	< 20	Very high	23.79	5
	20–40	High		4
	40–60	Moderate		3
	60–90	Low		2
	> 100	Very low		1
Elevation (m)	< 5	Very high	10.90	5
	5–10	High		4
	10–12	Moderate		3
	12–15	Low		2
	> 15	Very low		1
Slop (%)	0–2	Very high	12.28	5
	2–5	High		4
	5–8	Moderate		3
	8–15	Low		2
	> 15	Very low		1
Land use/land cover	Urban land	High	7.81	4
	Forest land	Low		2
	Agriculture land	Moderate		3
	Water bodies	Very high		5
Drainage density (km/km ²)	< 1	Very low	4.36	1
	1–2	Low		2
	3–3	Moderate		3
	3–4	High		4
	> 4	Very high		5
Soil	Sand	Extremely low	3.02	1
	Silty clay	Very high		4
	Sandy clay	High		3
	Clay	Extremely high		5
Lithology	Quaternary marine deposits	Low	2.61	1
	Quaternary alluvium/fluval	Moderate		2
	Charnockite	High		3

zones in the Chennai area. These eight layers were explored and digitally mapped using ArcGIS. The layers were used to demonstrate the following: precipitation as the primary source of water; distance to the river, determining effective infiltration zones; elevation, influencing overflow direction and water table depth; slope, controlling water flow intensity; LULC, impacting recharge processes; drainage density, governing runoff partitioning and infiltration rate; and soil properties affecting runoff partitioning and infiltration rate.

Factors influencing flood susceptibility zoning

Rainfall

Floods become more frequent as rainfall intensifies, particularly flash floods. The overall pattern of mean annual rainfall in the basin exhibits its highest values (300–700 mm per year) in the southern sections, gradually increasing in a southern gradient toward the sea. Rainfall, strongly linked to river

flow, stands as the primary precipitation element contributing to flooding (Subbarayan and Sivaranjani 2020; Das 2019). Floods can occur in semi-arid regions when a substantial amount of rain falls in a short period of time (Chakraborty and Mukhopadhyay 2019; Das 2019; Liuzzo et al. 2019; Paul

et al. 2019). Thus, five rainfall classes were categorized in the study region according to flood susceptibility factors as very high, high, moderate, low, and very low (Table 3). Flooding is more likely to occur in the southern parts of the research area compared to the northern parts (Fig. 2 a).

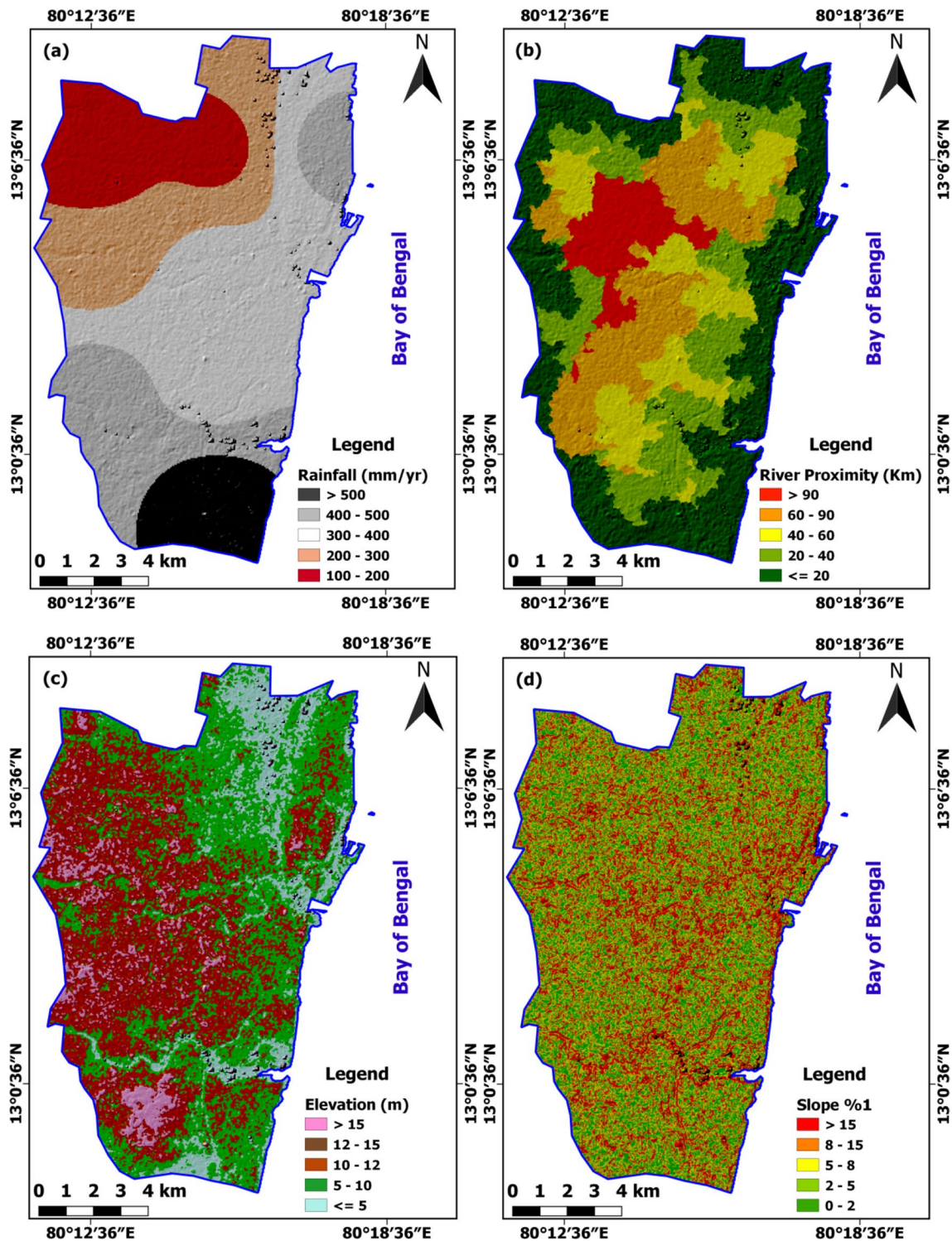


Fig. 2 The study area's **a** annual rainfall, **b** distance to rivers, **c** digital elevation model (DEM), and **d** slope map

Distance to the river

During floods, areas in close proximity to the rivers are more susceptible to the flooding risk (Xiao et al. 2017). The flooding risk increases due to the overcapacity of drainage channels, leading to their overflow and subsequent flooding. Areas adjacent to drainage canals are more likely to flood compared to areas farther away. Thus, locations near rivers were identified as more prone to flooding in the assessment (Fig. 2 b). Distances exceeding 20 km and ranging between 20 and 40 km from rivers are associated with a significant flooding risk. However, areas located at distances of 40–60 km, 60–90 km, and over 100 km from rivers are less likely to experience flooding.

Elevation

Flooding is more prevalent in low-lying areas when runoff changes from the high ground to the low ground. Rahman et al. (2019) claimed that low-lying areas are more vulnerable to flooding because even small floods can inundate them. Thus, the area with the lowest elevation (0–10 m above sea level) is the most vulnerable to flooding (Fig. 2 c). In contrast, some locations situated at elevations exceeding 15 m above sea level are less susceptible to flooding.

Slope

The slope of the ground influences the velocity and concentration of overland runoff. As the slope of a region increases, the likelihood of floods also rises, rendering it a valuable indicator of flooding vulnerability (Rahman et al. 2019). In general, steep slopes accelerate runoff, whereas gentle slopes can result in water stagnation and potential flooding (Dash and Sar 2020). According to Fig. 2 d, the study area was divided into five slope categories. Flood susceptibility is classified as very high (0–2%), high (2–5%), moderate (5–8%), low (8–15%), and very low (> 15%) (Table 3). Given that a significant portion of the basin lies within the floodplain (5%), the slope is fairly low. This type of slope, present throughout the area, characterized by the lowest slope and topographic elevation, holds the greatest importance among the variables contributing to flooding.

Land use/land cover

There are a variety of factors that influence LULC in the generation of surface runoff and flooding in a watershed (Sivakumar et al. 2017; Areu-Rangel et al. 2019; Khosravi et al. 2020). Infiltration rates, surface and groundwater interactions, evapotranspiration, and surface runoff formation are all influenced by LULC (Kazakis et al. 2015; Samanta et al. 2018;

Das 2019). Water bodies are particularly susceptible to flooding (Ogato et al. 2020), and in the current study, they were classified as having very high potential flood risk. Impervious land cover reduces infiltration capacity, and runoff from such areas contributes significantly to total runoff. Flooding is more likely in urbanized areas due to reduced lag time and increased total runoff resulting from urbanization. Rainfall affects bare soil in forested areas, making them more prone to flooding. A reaserch by Katie et al. (2010) has shown that raindrops can dissolve soil layers and create a surface crust, reducing infiltration rates and hydraulic conductivity, thereby increasing runoff and flood risk (Katie et al. 2010). Plant density and flooding are negatively correlated (Mojaddadi et al. 2017), implying that vegetated areas are less susceptible to flooding and therefore have lower flood risk scores. The degree of water and sediment flow facilitation at the pedon, slope, and watershed scale is termed connectivity (Keesstra et al. 2018). Agricultural fields have low connectivity due to their high roughness and high infiltration rates. According to Cerda et al. (2021), increased roughness results in a low runoff coefficient. Consequently, agricultural land has the lowest runoff coefficient and thus the highest susceptibility to flooding (Table 3). The urban land type is the most prevalent LULC type in the region, constituting over 90% of the study area (Fig. 3 a) and posing a significant flood risk.

Drainage density

The flood susceptibility is proportionate to drainage density, where increased drainage leads to higher runoff and greater flood vulnerability (Subbarayan and Sivaranjani 2020). There are five categories of drainage density in the area based on their impact on flood susceptibility: “very low” (> 1 km/km²), “low” (1–2 km/km²), “moderate” (2–3 km/km²), “high” (3–4 km/km²), and “very high” (< 4 km/km²). Accordingly, the majority of locations have low runoff density, indicating a minimal risk of flooding (Fig. 3 b).

Soil features

Figure 3 c shows a soil map of the study area, divided into four categories: sand, silty loam, sandy loam, and clay. In the northern part of the region, sand, silty loam, and sandy clay soil types are prevalent, constituting about 10% of the soil composition. Distinct soil types exhibit varying infiltration rates. Flooding becomes more likely when the infiltration capacity of the soil decreases, resulting in greater runoff. When rainfall exceeds the infiltration capacity of the soil, the excess rain runs down a slope and causes flooding (Lei et al. 2020). Soil pore size distribution, porosity, and pore connectivity can affect water movement. According to the results of the study, clay soils

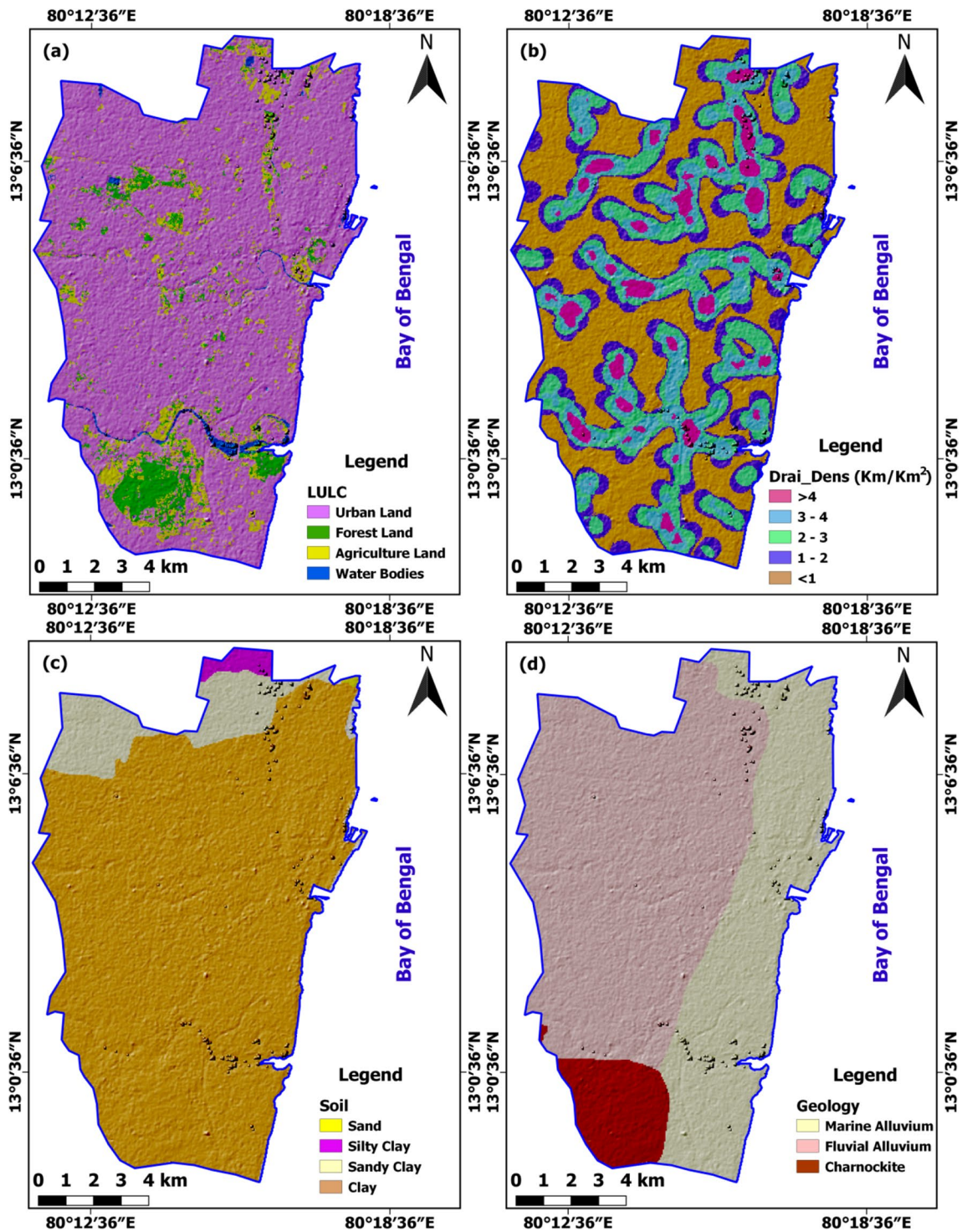


Fig. 3 The study area's **a** LULC, **b** drainage density, **c** soil type (dominant grain sizes), and **d** lithology map

account for more than 90% of the soil types in the study area and are classified as being at high or very high risk of flooding (Table 3).

Lithology

Three lithologic units are represented on the thematic map of Chennai district lithology: Quaternary marine

deposits, Quaternary alluvium and fluvial rocks, and charnockite igneous rocks (Fig. 3 d). The lithology of a site affects its capacity for infiltration and runoff (Dash and Sar 2020). Permeable lithology facilitates water penetration, while impermeable lithology contributes to surface runoff, potentially resulting in flooding. The region's eastern portions are covered by marine deposits, primarily composed of unconsolidated sediments from the Quaternary. The high porosity and permeability of these sediments render them as extremely low flood susceptibility zones. The majority of the western area is covered by Quaternary alluvium and river sedimentary strata, mainly representing the fluvial sediments of the Tigris and Euphrates Rivers, along with their tributaries. Due to their high porosity and permeability, these sediments are considered to have a very low flood risk (Table 3). Metamorphic and igneous rocks in the southernmost region have limited porosity and permeability, resulting in high runoff potential. These lithologies are classified as high to extremely high in the lithologic subclassification for flood risk. (Nasir et al. 2018; Kanagaraj et al. 2019) (Table 3). Conversely, evaporates are often associated with low porosity and permeability, as well as significant runoff potential (Earle 2019), and are ranked as very high in the lithologic subclassification for flood risk.

Flood susceptibility zoning

Using the eight flood susceptibility mapping factors, a flood susceptibility map was created with four distinct classes (zones) (Fig. 4). The area represents high, moderate, low, and extremely low vulnerability to flood hazards, occupying 16.41%, 67.33%, 16.18%, and 0.08% of the total area, respectively. In general, regions prone to flood hazards and areas with high runoff exhibit a wide range of contributing factors. High flood risk zones are primarily located in the southern part, while moderate flood risk areas are concentrated in the central portion of the study area. Regions with the lowest and very low flood risk are predominantly found in the northwest and north (Fig. 4). For locations classified as having “high susceptibility”, favorable factors include DEM, slope, and drainage density. Proximity to rivers, low DEM, and high drainage density contribute to increased vulnerability to flood hazards. In the southern parts of the area, low drainage density and high DEM mitigate most rainfall, leading to transformation of high flood risk areas into moderate ones. In contrast, the western and northwestern regions face the least flood risk due to their low rainfall,

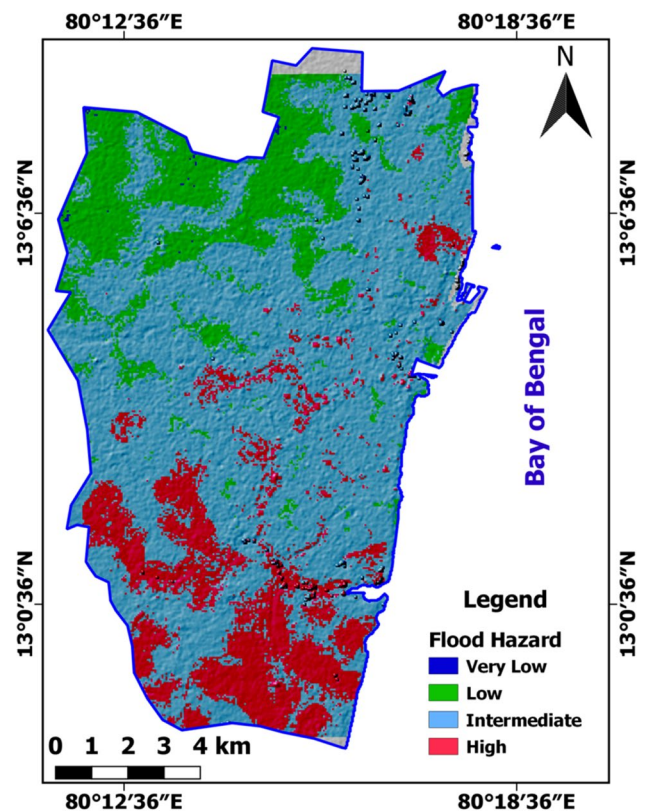


Fig. 4 Map showing final flood susceptibility zones, Chennai, India

drainage density and their distance from rivers, elevation, and slope. Consequently, runoff per unit area decreases with increasing slope length due to the combined effects of infiltration and runoff from ponding (Zhao et al. 2018; Cerda et al. 2021). Runoff from the upper slopes of dry regions does not reach river channels due to infiltration, resulting in its isolation from the drainage system. As a consequence, only runoff generated during specific events in areas around the channels reaches the river channel and triggers flooding (Cerda et al. 2021).

Limitation of the study and suggestion

There are several factors contributing to more frequent and intense flooding in the Chennai watershed, including significant changes in runoff across the district. The AHP technique created a mathematically structured ranking of options. This strategy decomposed a complex selection problem into three components: a target, criteria, and options. Given that flooding cannot be prevented or stopped, it is best to minimize its impact and destruction and select

options. Expert comments from a consultation questionnaire are then used to make pairwise comparisons between each parameter and its alternatives to assess the relative relevance of each parameter (Elkhrachy 2015). However, flood hazard vulnerability assessments are based on direct measurements in the area (Lyu et al. 2020). In the context of flood risk assessment, this may not be practical because researchers have focused on the lack of use of data in AHP (Danumah et al. 2016; Gigovic et al. 2017; Cabrera and Lee 2019). As a measure, this study used remote sensing-GIS and AHP approach to provide an effective method for appropriate identification of flood risk zones. This study confirmed that AHP is able to accurately predict flood hazards and map risk zones, in the Chennai area. The flood risk map produced was an effective choice for reducing flood risk in flood-prone areas. As the outcome of AHP relies on expert judgment, it can be susceptible to intellectual limitations arising from subjectivity and ambiguity.

The basic AHP uses a single number to reflect the decision maker's preference for one of the options in a pairwise comparison. On the other hand, a concise value may not adequately reflect the decision maker's point of view. In addition, it is time-consuming for the AHP approach to solicit ratings from numerous experts using its standard questionnaire. The evaluation matrix often contains inconsistencies as individuals' subjective preferences are considered in pairwise comparisons (Lyu et al. 2020). Considering the results of this study, flood damage to people and infrastructure can be prevented in the future. Although the AHP method for determining the relative importance of components has some advantages, it also has some disadvantages. The typical AHP approach may be sufficient for differentiating development opportunities in the early stages of the planning process.

More complex methods, on the other hand, are preferable when calculating the specific area of the desired growth region. The fuzzy method has been used for more detailed analysis of flood susceptibility (Radmehr and Araghinejad 2015; Sahana and Patel 2019). The combination of AHP with the fuzzy method has been used for land use planning (Mosadeghi et al. 2015), groundwater potential zone modeling (Mallick et al. 2019), and geohazard vulnerability assessment (Zheng et al. 2021). It is believed that the AHP fuzzy method can also increase the accuracy of flood vulnerability mapping.

The weights of the AHP parameters are determined by the experience of the experts and might lead to potential errors. Therefore, optimization methods or artificial intelligence (AI) methods are required for objectively determining the weights of the AHP parameters. Hybrid AI methods and metaheuristic optimization methods

have been used for flood vulnerability modeling (Bui et al. 2016). Integration of swarm optimization with deep learning neural networks was used for flood susceptibility mapping (Bui et al. 2020). Coupling an adaptive neuro-fuzzy inference system (ANFIS) with a genetic algorithm and a differential evolution method was also used for flood susceptibility assessment (Hong et al. 2018). For future planning efforts, the AHP strategy needs to be used in conjunction with fuzzy methods, optimization methods, or AI methods to obtain a more accurate assessment of flood vulnerability in the study area. This study was a preliminary assessment of flood-prone areas in a watershed for which a standard AHP approach was used.

Recommendations

GIS-MCDA is a valuable flood risk management tool because it can help identify flood-prone areas, evaluate the effectiveness of flood control strategies, and assess the vulnerability of different populations to flooding. By providing decision makers with comprehensive information on the potential impacts of flooding and the effectiveness of various strategies, GIS-MCDA can support the development of effective and efficient flood risk management plans. In general, here are some suggestions for effective flood risk management based on previous findings and this study: (1) Identify the most vulnerable areas by mapping land use, population density, and other geospatial data. This information can be used to set priorities for implementing flood management strategies. (2) Develop a comprehensive understanding of the potential impacts of flooding, including potential loss of life, damage to infrastructure and property, and disruption to transportation and commerce. This information can be used to evaluate the effectiveness of various flood management strategies and prioritize actions. (3) Implement flood management strategies tailored to the specific needs of different populations, such as low-income households or people with limited access to transportation. Targeted actions can help reduce flood risk and mitigate the impact of flooding on vulnerable populations. (4) Use GIS-MCDA to regularly evaluate the effectiveness of flood management strategies and adjust them as needed. This model can help ensure that resources are used efficiently and effectively to reduce flood risk. (5) Encourage collaboration among various stakeholders, including government agencies, community organizations, and private businesses, to develop and implement effective flood management strategies.

Conclusions

The MCDA framework, combined with AHP approach applied at the watershed level, proved useful for identifying vulnerable zones to flood hazards in the Chennai area, India. For flood hazard vulnerability mapping, an assemblage of datasets encompassing rainfall, topography, geology, soils, land use, and drainage density were compiled and inserted into the MCDA framework for the purpose of assigning weights to each contributing factor in flood susceptibility mapping. The resulting map showed that the southern parts of Chennai are particularly vulnerable to flooding. The upstream and downstream parts of the area are often less susceptible to flooding. The results showed that locations near rivers, low elevation and slope, and high runoff density are particularly vulnerable due to their higher probability of flooding. The optimal weighting of components contributing to flood risk was calculated based on expert judgments and expertise using AHP technique. AHP method was found to be accurate by comparing the results with historical flood data and flood models. Because the technique is versatile, easy to use, and inexpensive, it can be realistically applied, especially to case studies with limited information and data. Despite its advantages, the traditional AHP also has some disadvantages. Considering the history of floods in the study area, the traditional AHP technique is sufficient. However, it is suggested to combine the AHP method with fuzzy methods, optimization methods, or AI methods to obtain more successful results for future planning. This study provides a preliminary flood risk prediction for local emergency management authorities, planners, researchers, and agencies interested in flood hazard management.

Acknowledgements This research was supported by the Basic Science Research Program through the National Research Foundation of Korea (NRF) funded by the Ministry of Education (2019R1D1A3A03103683).

Author contribution Murugesan Bagyaraj: Original draft, data collection, formal analysis, writing.

Venkatramanan Senapathi: Original draft, data collection, formal analysis, writing, project administration.

Sang Yong Chung: Original draft, data collection, formal analysis, writing, project administration.

Gnanachandrasamy Gopalakrishnan: Writing–review and editing, visualization.

Yong Xiao: Writing–review and editing, visualization, supervision.

Sivakumar Karthikeyan: Data collection, resources, software, writing–review and editing.

Ata Allah Nadiri: Writing–review and editing, data collection, resources, software, visualization.

Rahim Barzegar: Writing–review and editing.

Funding The authors are grateful to the Department of Environment's Laboratory (Chittagong Office) for providing all necessary support during lab activities. This research received the full funding from the Basic Science Research Program through the National Research Foundation of Korea (NRF) funded by the Ministry of Education, Korea.

Data availability The authors are grateful to the Department of Environment's Laboratory (Chittagong Office) for providing all necessary support during lab activities. Data are available from the authors upon reasonable request and with permission of National Research Foundation, Korea 451 (KNRF).

Declarations

Ethics approval Not applicable.

Consent to participate Not applicable.

Consent to publish Not applicable.

Competing interests The authors declare no competing interests.

References

- Agastheeswaran V, Udayaganesan P, Sivakumar K, Venkatramanan S, Prasanna MV, Selvam S (2021) Identification of groundwater potential zones using geospatial approach in Sivagangai district, South India. *Arabian J Geosci* 14(1):8. <https://doi.org/10.1007/s12517-020-06316-4>
- Areu-Rangel O, Cea L, Bonasia R, Espinosa-Echavarria V (2019) Impact of urban growth and changes in land use on river flood susceptibility in Villahermosa, Tabasco (Mexico). *Water (switzerland)* 11(2):304–315
- Arshad A, Zhang Z, Zhang W, Dilawar A (2020) Mapping favorable groundwater potential recharge zones using a GIS-based analytical hierarchical process and probability frequency ratio model: a case study from an agro-urban region of Pakistan. *Geosci Front* 11(5):1805–1819
- Barasa N, Perera E (2018) Analysis of land use change impacts on flash flood occurrences in the Sosiani River basin Kenya Betty. *Int J River Basin Manag* 16(2):179–188
- Brunelli M (2015) Introduction to the analytic hierarchy process. Springer, New York
- Bui DT, Pradhan B, Nampak H, Bui QT, Tran QA, Nguyen QP (2016) Hybrid artificial intelligence approach based on neural fuzzy inference model and metaheuristic optimization for flood susceptibility modeling in a high-frequency tropical cyclone area using GIS. *J Hydrol* 540:317–330. <https://doi.org/10.1016/j.jhydrol.2016.06.027>
- Bui QT, Nguyen QH, Nguyen XL, Pham VD, Nguyen HD, Pham VM (2020) Verification of novel integrations of swarm intelligence algorithms into deep learning neural network for flood susceptibility mapping. *J Hydrol* 581:124379. <https://doi.org/10.1016/j.jhydrol.2019.124379>
- Cabrera JS, Lee HS (2019) Flood-prone area assessment using GIS-based multi-criteria analysis: a case study in Davao Oriental, Philippines. *Water* 11:2203
- CCC&AR and TNSCCC (2015) Climate change projection (rainfall) for Chennai. In: District-Wise Climate Change Information for the State of Tamil Nadu. Centre for Climate Change and Adaptation Research (CCC&AR), Anna University and Tamil Nadu State Climate Change Cell (TNSCCC), Department of Environment (DoE), Government of Tamil Nadu, Chennai, Tamil Nadu, India. Available at URL. www.tnsccc.in. Accessed 20 Dec 2022
- Cerda A, Novara A, Dlapa P, Lopez-Vicente M, Ubeda X, Popovic Z, Mekonnen M, Terol E, Janizadeh S, Mbarki S et al (2021) Rainfall and water yield in Macizo del Caroig, Eastern Iberian Peninsula. Event runoff at plot scale during a rare flash flood at the Barranco de Benacancil. *CIG* 47(1):95–119

- Chakraborty S, Mukhopadhyay S (2019) Assessing flood risk using analytical hierarchy process (AHP) and geographical information system (GIS): application in Coochbehar district of West Bengal. *Nat Susceptibility* 99(1):247–274
- Chomba IC, Banda KE, Winsemius HC, Chomba MJ, Mataa M, Ngwenya V, Sichingabula HM, Nyambe IA, Ellender B (2021) A review of coupled hydrologic-hydraulic models for floodplain assessments in Africa: opportunities and challenges for floodplain wetland management. *Hydrology* 8:44. <https://doi.org/10.3390/hydrology8010044>
- Danumah JH, Odai SN, Saley BM, Szarzynski J, Thiel M, Kwaku A, Kouame FK, Akpa LY (2016) Flood risk assessment and mapping in Abidjan district using multi-criteria analysis (AHP) model and geoinformation techniques, (cote d'ivoire). *Geoenviro Disasters* 3:10
- Das S (2019) Geospatial mapping of flood susceptibility and hydrogeomorphic response to the floods in Ulhas basin, India. *Remote Sens Appl Soc Environ* 14:60–74
- Dash P, Sar J (2020) Identification and validation of potential flood susceptibility area using GISbased multi-criteria analysis and satellite data-derived water index. *J Flood Risk Manag* 13(3):e12620
- de Brito MM, Evers M (2016) Multi-criteria decision-making for flood risk management: a survey of the current state of the art. *Nat Susceptibility Earth Syst Sci* 16(4):1019–1033
- de Moel H, Jongman B, Kreibich H (2015) Flood risk assessments at different spatial scales. *Mitig Adapt Strateg Glob Chang* 20:865–890. <https://doi.org/10.1007/s11027-015-9654-z>
- Deng Z, Zhang X, Li D, Pan G (2015) Simulation of land use/land cover change and its effects on the hydrological characteristics of the upper reaches of the Hanjiang Basin. *Environ Earth Sci* 73(3):1119–1132
- Detrembleur S, Stilmant F, Dewals B, Ercpicum S, Archambeau P, Pirotton M (2015) Impacts of climate change on future flood damage on the river Meuse, with a distributed uncertainty analysis. *Nat Susceptibility* 77(3):1533–1549
- Dou X, Song J, Wang L, Tang B, Xu S, Kong F, Jiang X (2018) Flood risk assessment and mapping based on a modified multi-parameter flood susceptibility index model in the Guanzhong Urban Area. *Stoch Environ Res Risk Assess* 32(4):1131–1146
- Earle S (2019) *Physical geology*. 2nd ed. Victoria, B.C.: BCcampus. <https://opentextbc.ca/physicalgeology2ed/>. Accessed 17 Feb 2022
- Elkhrachy I (2015) Flash flood susceptibility mapping using satellite images and GIS tools: a case study of Najran City, Kingdom of Saudi Arabia (KSA). *Egypt J Remote Sens Space Sci* 18(2):261–278
- Feizizadeh B, Blaschke T, Shadman RM (2013) Integrating GIS based fuzzy set theory in multicriteria evaluation methods for landslide susceptibility mapping. *Int J Geoinf* 9:49–57
- Ghosh A, Kar S (2018) Application of analytical hierarchy process (AHP) for flood risk assessment: a case study in Malda district of West Bengal. *Nat Susceptibility* 94(1):349–368
- Gigovic L, Pamucar D, Bajic Z, Drobnjak S (2017) Application of GIS-Interval rough AHP methodology for flood susceptibility mapping in urban areas. *Water* 9(6):360–326
- Goepel K (2013) Implementing the analytic hierarchy process as a standard method for multicriteria decision making in corporate enterprises – a new AHP excel template with multiple inputs. *Proceedings of the International Symposium on the Analytic Hierarchy Process*, Kuala Lumpur, 2013 <https://doi.org/10.13033/isahp.y2013.047>
- Hirabayashi Y, Alifu H, Yamazaki D, Imada Y, Shiogama H, Kimura Y (2021) Anthropogenic climate change has changed frequency of past flood during 2010–2013. *Abstract Progress in Earth and Planetary Science* 8(1). <https://doi.org/10.1186/s40645-021-00431-w>
- Hong H, Panahi M, Shirzadi A, Ma T, Liu J, Zhu AX, Chen W, Kougias I, Kazakis N (2018) Flood susceptibility assessment in Hengfeng area coupling adaptive neuro-fuzzy inference system with genetic algorithm and differential evolution. *Sci Total Environ* 621:1124–1141. <https://doi.org/10.1016/j.scitotenv.2017.10.114>
- Joy J, Kanga S, Singh SK (2019) Kerala flood 2018: flood mapping by participatory GIS approach, Meloor Panchayat. *Int J Emerg Technol* 10(1):197–205
- Kachouri S, Achour H, Abida H, Bouaziz S (2015) Soil erosion susceptibility mapping using analytic hierarchy process and logistic regression: a case study of Haffouz watershed, Central Tunisia. *Arab J Geosci* 8(6):4257–4268
- Kanagaraj G, Suganthi S, Elango L, Magesh N (2019) Assessment of groundwater potential zones in Vellore district, Tamil Nadu, India using geospatial techniques. *Earth Sci Inform* 12(2):211–223
- Katie P, Jackson CR, Parker AJ (2010) Variation of surficial soil hydraulic properties across land uses in the southern Blue Ridge Mountains North Carolina USA. *Journal of Hydrology* 383(3–4):256–268. <https://doi.org/10.1016/j.jhydrol.2009.12.041>
- Kazakis N, Kougias I, Patsialis T (2015) Assessment of flood susceptibility areas at a regional scale using an index-based approach and analytical hierarchy process: application in RhodopeEvros region, Greece. *Sci Total Environ* 538:555–563
- Keesstra S, Nunes J, Saco P, Parsons T, Poepl R, Masselink R, Cerda A (2018) The way forward: can connectivity be useful to design better measuring and modelling schemes for water and sediment dynamics? *Sci Total Environ* 644:1557–1572
- Khosravi K, Panahi M, Golkarian A, Keesstra SD, Saco PM, Bui DT, Lee S (2020) Convolutional neural network approach for spatial prediction of flood susceptibility at national scale of Iran. *J Hydrol* 591:125552
- Kongeswaran T, Sivakumar K (2022) Application of remote sensing and GIS in floodwater harvesting for groundwater development in the Upper Delta of Cauvery River Basin, Southern India. In Pankaj K, Gaurav KN, Manish Kumar S, Anju S (Eds.), *Water Resources Management and Sustainability, Advances in Geographical and Environmental Sciences*. Springer Nature, pp. 257–280 https://doi.org/10.1007/978-981-16-6573-8_14
- Kuldeep Garg PK, Garg RD (2016) Geospatial techniques for flood inundation mapping. 2016 IEEE International Geoscience and Remote Sensing Symposium (IGARSS). p. 4387–4390
- Kumar V, Mondal N, Ahmed S (2020) Identification of groundwater potential zones using RS, GIS and AHP techniques: a case study in a part of Deccan Volcanic Province (DVP), Maharashtra, India. *J Indian Soc Remote Sens* 48(3):497–511
- Lei W, Dong H, Chen P, Lv H, Fan L, Mei G (2020) Study on runoff and infiltration for expansive soil slopes in simulated rainfall. *Water*. 12(1):222. www.mdpi.com/journal/water. Accessed 30 Mar 2021
- Liu Z, Zhang H, Liang Q (2018) A coupled hydrological and hydrodynamic model for flood simulation. *Hydrol Res* (2019) 50(2):589–606. <https://doi.org/10.2166/nh.2018.090>
- Liuzzo L, Sammartano V, Freni G (2019) Comparison between different distributed methods for flood susceptibility mapping. *Water Resour Manag* 33(9):3155–3173
- Lyu HM, Shen SL, Zhou A, Yang J (2020) Risk assessment of mega-city infrastructures related to land subsidence using improved trapezoidal FAHP. *Sci Total Environ* 717:135310
- Mallick J, Khan R, Ahmed M, Alqadhi S, Alsubih M, Falqi I, Abul HM (2019) Modeling groundwater potential zone in a semi-arid region of aseer using fuzzy-AHP and geoinformation techniques. *Water* 11(12):2656
- Mojaddadi H, Pradhan B, Nampak H, Ahmad N, Ghazali AH (2017) Ensemble machine-learning-based geospatial approach for flood risk assessment using multi-sensor remote-sensing data and GIS Geomatics. *Nat Susceptibility Risk* 8(2):1080–1102
- Mosadeghi R, Warnken J, Tomlinson R, Mirfenderesk H (2015) Comparison of Fuzzy-AHP and AHP in a spatial multi-criteria decision making model for urban land-use planning. *Comput Environ Urban Syst* 49:54–65

- Muthusamy S, Sivakumar K, Durai AS, Sheriff MR, Subramanian PS (2018) Ockhi cyclone and its impact in the Kanyakumari District of Southern Tamilnadu, India : an aftermath analysis. *International Journal of Recent Research Aspects*, April, 466–469. https://www.ijrra.net/April2018/ConsComp2018_110.pdf. Accessed 27 July 2018
- Naghibi S, Pourghasemi H, Pourtaghi Z, Rezaei A (2015) Groundwater qanat potential mapping using frequency ratio and Shannon's entropy models in the Moghan watershed, Iran. *Earth Sci Inform* 8(1):171–186
- Nasir M, Khan S, Zahid H, Khan A (2018) Delineation of groundwater potential zones using GIS and multi influence factor (MIF) techniques: a study of district Swat, Khyber Pakhtunkhwa, Pakistan. *Environ Earth Sci* 77(10):1–11
- Ogato G, Bantider A, Abebe K, Geneletti D (2020) Geographic information system (GIS)-based multicriteria analysis of flooding susceptibility and risk in Ambo Town and its watershed, West shoa zone, oromia regional State Ethiopia. *J Hydrol Regional Studies* 27(2020):100659
- Paul GC, Saha S, Hembram TK (2019) Application of the GIS-based probabilistic models for mapping the flood susceptibility in Bansloi sub-basin of Ganga-Bhagirathi River and their comparison. *Remote Sens Earth Syst Sci* 2(2–3):120–146
- Prabakaran K, Sivakumar K, Aruna C (2020) Use of GIS-AHP tools for potable groundwater potential zone investigations—a case study in Vairavanpatti rural area, Tamil Nadu, India. *Arabian J Geosci* 13(17):866. <https://doi.org/10.1007/s12517-020-05794-w>
- Radmehr A, Araghinejad S (2015) Flood vulnerability analysis by fuzzy spatial multi criteria decision making. *Water Resour Manag* 29(12):4427–4445
- Rahman M, Ningsheng C, Islam M, Dewan A, Iqbal J, Washakh R, Shufeng T (2019) Flood susceptibility assessment in Bangladesh using machine learning and multi criteria decision analysis. *Earth Syst Environ* 3(3):585–601
- Rahmati O, Pourghasemi HR, Zeinivand H (2016a) Flood susceptibility mapping using frequency ratio and weights-of-evidence models in the Golastan Province, Iran. *Geocarto Int* 31(1):42–70
- Rahmati O, Zeinivand H, Besharat M (2016b) Flood susceptibility zoning in Yasooj region, Iran, using GIS and multi-criteria decision analysis. *Geomatics Nat Susceptibility Risk* 7(3):1000–1017
- Rimba AB, Setiawati MD, Sambah AB, Miura F (2017) Physical flood vulnerability mapping applying geospatial techniques in Okazaki City, Aichi Prefecture. *Japan Urban Sci* 1(1):7–22
- Saaty T (1980) The analytic hierarchy process (AHP) for decision making. In: Kobe, vol 1, Japan, p 69
- Saaty T (2014) *Decision making for leaders: the analytic hierarchy process for decisions in a complex world*. RWS Publications, Pittsburgh, PA, USA
- Sahana M, Patel PP (2019) A comparison of frequency ratio and fuzzy logic models for flood susceptibility assessment of the lower Kosi River Basin in India. *Environ Earth Sci* 78(10):1
- Samanta RK, Bhunia GS, Shit PK, Pourghasemi HR (2018) Flood susceptibility mapping using geospatial frequency ratio technique: a case study of Subarnarekha River Basin. *Model Earth Syst Environ* 4(1):395–408
- Seejata K, Yodying A, Wongthadam T, Mahavik N, Tantane S (2018) Assessment of flood susceptibility areas using analytical hierarchy process over the Lower Yom Basin, Sukhothai Province. *Procedia Eng* 212:340–347
- Sindhu K, Durga Rao KHV (2017) Hydrological and hydrodynamic modeling for flood damage mitigation in Brahmani-Baitarani River Basin, India. *Geocarto Int* 32(9):1004–1016. <https://doi.org/10.1080/10106049.2016.1178818>
- Sivakumar K, Muthusamy S, Jayaprakash M, Mohana P, Sudharson ER (2017) Application of post classification in landuse & landcover stratagies at north Chennai industrial area. *Journal of Advanced Research in Geo Sciences & Remote Sensing*, 4(3&4):1–13. <http://thejournalshouse.com/index.php/geoscience-remotesensing-earth/article/download/239/59>. Accessed 29 Nov 2017
- Subbarayan S, Sivaranjani S (2020) Modelling of flood susceptibility based on GIS and analytical hierarchy process—a case study of Adayar River Basin, Tamilnadu, India. In: Pal I, von Meding J, Shrestha S, Ahmed I, Gajendran T (eds) *An interdisciplinary approach for disaster resilience and sustainability*. MRDRRE 2017. *Disaster Risk Reduction (Methods, Approaches and Practices)*. Springer, Singapore
- Tabari H (2020) Climate change impact on flood and extreme precipitation increases with water availability. *Sci Rep* 10(1):13768
- Ullah S, Farooq M, Sarwar T, Tareen MJ, Wahid MA (2016) Flood modeling and simulations using hydrodynamic model and ASTER DEM—a case study of Kalpani River. *Arab J Geosci* 9(6):439
- Vieri T, Giovanni M, Maurizio R, Maurizio T, Alessandro P, Mohamed HI, Gaptia L, Katiellou Paolo T, De Filippis T, Leandro R, Valentina M, Elena R (2020) Community and impact based early warning system for flood risk preparedness: the experience of the Sirba River in Niger. *Sustainability* 12:1802. <https://doi.org/10.3390/su12051802>
- Wu Y, Zhong P, Zhang Y, Xu B, Ma B, Yan K (2015) Integrated flood risk assessment and zonation method: a case study in Huaihe River basin. *Nat Susceptibility Risk* 7(1):635–651
- Xiao Y, Yi S, Tang Z (2017) Integrated flood susceptibility assessment based on spatial ordered weighted averaging method considering spatial heterogeneity of risk preference. *Sci Total Environ* 599–600(2017):1034–1046
- Yan B, Fang NF, Zhang PC, Shi ZH (2013) Impacts of land use change on watershed streamflow and sediment yield: an assessment using hydrologic modelling and partial least squares regression. *J Hydrol* 484:26–37
- Zhang J, Chen Y (2019) Risk Assessment of Flood Disaster Induced by Typhoon Rainstorms in Guangdong Province China. *Sustainability* 11(10):2738. <https://doi.org/10.3390/su11102738>
- Zhao L, Hou R, Wu F, Keesstra S (2018) Effect of soil surface roughness on infiltration water, ponding and runoff on tilled soils under rainfall simulation experiments. *Soil Tillage Res* 179:47–53
- Zheng Q, Lyu HM, Zhou A, Shen SL (2021) Risk assessment of geosusceptibility along Cheng-Kun railway using fuzzy. AHP Incorporated into GIS. *Geomatics Nat Susceptibility Risk* 12(1):1508–1531

Publisher's note Springer Nature remains neutral with regard to jurisdictional claims in published maps and institutional affiliations.

Springer Nature or its licensor (e.g. a society or other partner) holds exclusive rights to this article under a publishing agreement with the author(s) or other rightsholder(s); author self-archiving of the accepted manuscript version of this article is solely governed by the terms of such publishing agreement and applicable law.